

## The Relationship Between Structure and Second Hyperpolarisability in Conjugated Hydrocarbons

Robert Thomas

Laboratorium für Organische Chemie, ETH-Zürich, Universitätstrasse 16, 8092-Zürich, Switzerland

The well known correlation between molecular length and second hyperpolarisability,  $\gamma$ , in linear conjugated oligomers is extended to include curved aromatic molecules by considering the surface area rather than length. The new relationship provides a means of comparing hydrocarbons of widely differing structure, as well as indicating the onset of the saturation limit found in linear polymers. The application to the design of materials with high non-linear optical responses is discussed.

The interdisciplinary field of non-linear optics (NLO) has shown dramatic growth in the three decades since the discovery of lasers made these effects easier to investigate.<sup>1</sup> The significance of organic materials in this area is highlighted by the number of reviews on the subject that have appeared in recent years.<sup>2</sup> Relationships between molecular structure and the magnitude of the NLO response is of singular importance for the rational design of new and improved materials.<sup>2a</sup> This is particularly so of the second hyperpolarisability,  $\gamma$ ,\* for which no generally applicable structure-activity relationships are available.

The dipole moment,  $\mu$ , of a molecule in an electric field,  $F$ , can be written as the Taylor series:

$$\mu = \mu^0 + \alpha_{ij}F_j + (1/2)\beta_{ijk}F_jF_k + (1/6)\gamma_{ijkl}F_jF_kF_l + \dots$$

where  $\mu^0$  is the permanent dipole moment and  $\alpha_{ij}$ ,  $\beta_{ijk}$  and  $\gamma_{ijkl}$  are the tensor elements of the linear polarisability and first and second hyperpolarisabilities, respectively. The second hyperpolarisability,  $\gamma$  is responsible for third-order NLO effects such as third-harmonic generation, degenerate four-wave mixing, self focusing and the optical Kerr effect.<sup>2c</sup>

Following the work of Rustagi and Ducuing,<sup>3</sup> a number of theoretical and empirical correlations between  $\gamma$  and conjugation length ( $N$ ) have been proposed for oligomeric linear molecules such as polyenes. Often the conjugation length,  $N$ , is replaced by the number of  $\pi$  electrons,  $N_\pi$ , since these two values are proportional to one another in these linear systems. For each class of oligomer a relationship of the form  $\gamma \propto N^a$  ( $a > 1$ ) is found, though the exponent varies significantly both between oligomer series and as  $N$  becomes large.<sup>2a</sup> Theoretical and experimental studies have shown that for larger linear polymers a 'saturation regime' is entered where  $\gamma \propto N$  ( $a \approx 1$ ). In polyacetylenes this occurs at 50–60 carbon atoms,<sup>5</sup> for oligothiophenes it is at seven–eight rings.<sup>4</sup>

For comparisons between more diverse hydrocarbons, the second hyperpolarisability per carbon atom (actually  $\gamma/N_\pi$ ) is often used.<sup>6,2d</sup> These comparisons indicate that for a particular number of conjugated carbon atoms,  $\gamma$  is higher for linear polymers (quasi-one-dimensional) than for other systems. No coherent and synthetically useful picture has emerged to relate these differences in  $\gamma/N_\pi$  to structural differences among the molecules in question.

Herein will be described a simple relationship which unifies the description of  $\gamma$  for molecules of widely different structures and yields predictions about the saturation behaviour found in linear polymers.

### Calculations and Discussion

Examination of the literature<sup>2</sup> suggests that accurate calculation of  $\gamma$  can only be carried out using expensive *ab initio* techniques. However, since these become unfeasible for larger molecules, a great deal of attention has been drawn to semiempirical methods. Although not as accurate, values deviating by about 40–50% from empirical data can be obtained, and this level of agreement is viewed as good<sup>11</sup> to excellent.<sup>2b</sup> Semiempirical calculations were made using MOPAC 6.10<sup>7</sup> on a SGI Crimson Elan workstation. The MNDO Hamiltonian<sup>8</sup> with PM3 parametrisation<sup>9</sup> was used, as was Eigenvector Following.<sup>10</sup> The SCF convergence criterion was set at  $1.0 \times 10^{-20}$ . A finite field approach employing both energy expansion and dipole expansion was used to calculate the response of the charge density to the field.<sup>11</sup> Since the precision of the hyperpolarisability calculations has been improved in MOPAC 6, eleven aromatic molecules were calculated for comparison with the results of Dixon<sup>6</sup> running MOPAC 5; in all cases  $\Delta_rH$ , HOMO, LUMO, geometries, and polarisabilities were in agreement but second order hyperpolarisabilities,  $\gamma, \dagger$  were in all cases higher than those given by Dixon, and, where known, closer to the experimentally determined values at zero frequency.<sup>6</sup>

In order to concentrate on the effects of topology (and particularly curvature) without the complication of polarisation by heteroatoms we concentrated on three classes of fully conjugated hydrocarbons (in which all carbons are  $sp^2$  hybridised): Table 1 shows the results for the *cis*-polyacetylenes,  $C_nH_{n+2}$  ( $n = 2, 4, 6, 10, 20, 30, 40$  and  $50$ ), **1–8**; the linear acenes, from benzene, **9**, to hexacene **14**; and the group of 21 aromatic molecules (hereafter called curved aromatics) shown in Fig. 1. This group of aromatic molecules, the fullerenes  $C_{60}$  and  $C_{70}$ , and some of their molecular fragments were chosen to represent 'three-dimensional' molecules. A notable feature of this group is the trend found for  $\gamma$  as the molecular fragments are built up towards the parent fullerenes (for example the  $C_{60}$  series: **15, 21, 28, 30** and **32**). It is found that  $\gamma$  increases with  $N_\pi$  until the molecules are approximately hemispherical and then begins to decrease as the spheroid is completed. This is shown for the  $C_{60}$  series in Fig. 2.

As can be seen from the plot in Fig. 3, the polyacetylenes (red) and acenes (green) both show power relationships between the number of  $\pi$  electrons ( $N_\pi$ ) and  $\gamma$ . However, results for one series cannot be extrapolated to make predictions about the other. Furthermore, the early behaviour in a series gives little information about the onset of saturation. It is left to direct observation or calculation to determine this feature. Most importantly, the vast majority of compounds, those which are

\*  $\gamma = 1/5\{\gamma_{xxxx} + \gamma_{yyyy} + \gamma_{zzzz} + 2[\gamma_{xxyy} + \gamma_{xxzz} + \gamma_{yyzz}]\}$  is the orientationally averaged second hyperpolarisability at zero frequency.

† Throughout this discussion  $\gamma$  is taken to be in au ( $5.0367 \times 10^{-40}$  esu).

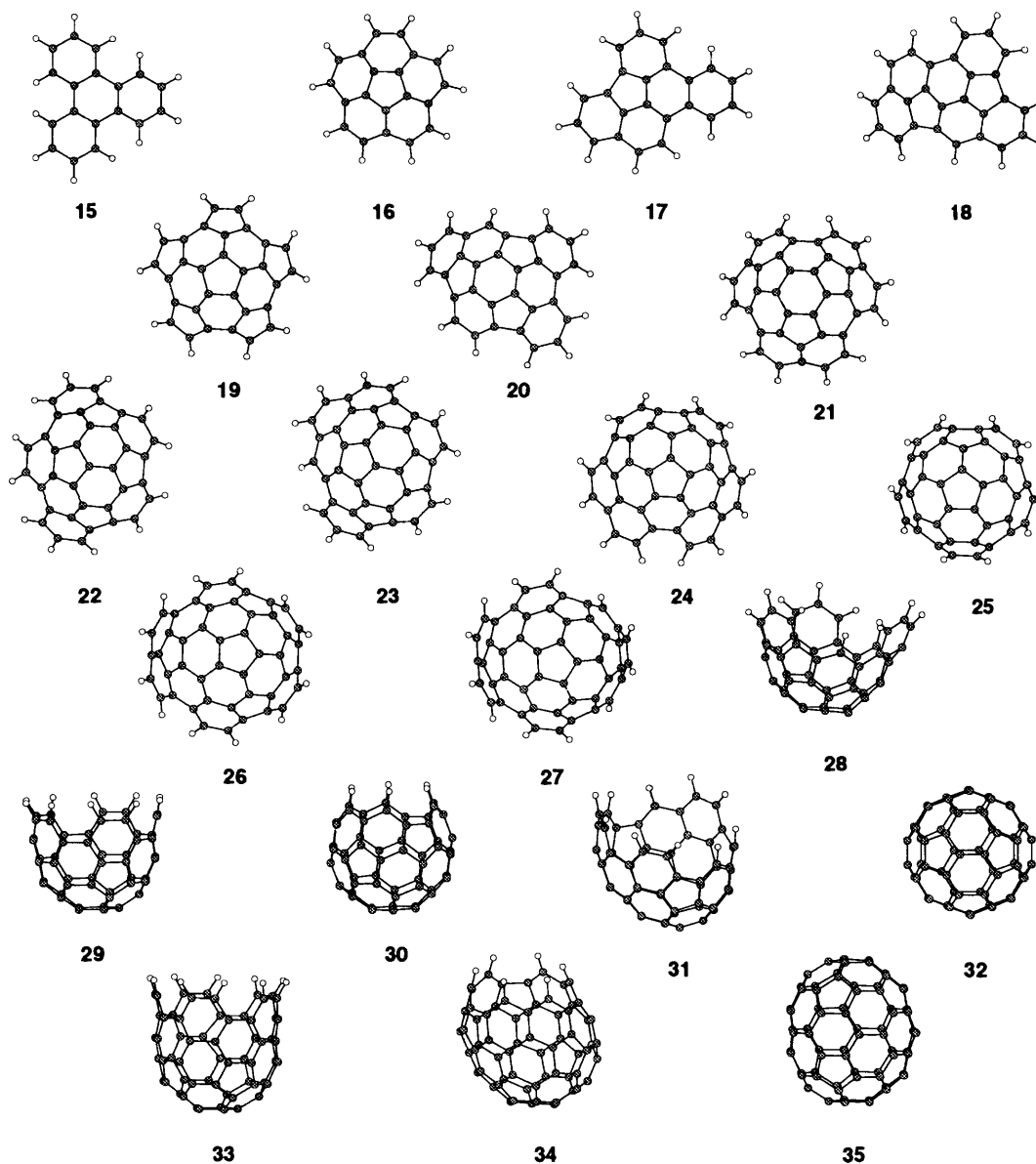


Fig. 1 Aromatic fragments of the fullerenes  $C_{60}$  and  $C_{70}$  chosen to represent 'three-dimensional' molecules

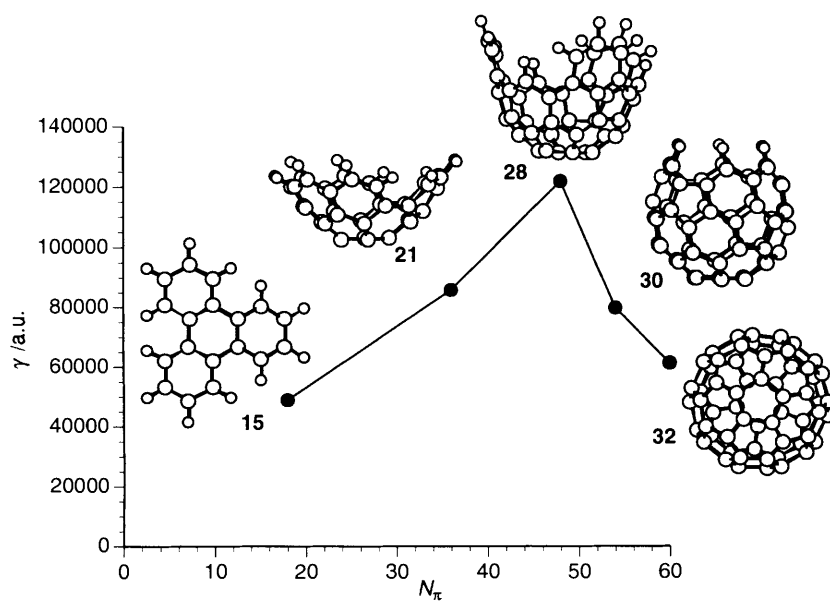


Fig. 2 The development of  $\gamma$  as aromatic fragments are built up towards the fullerene,  $C_{60}$

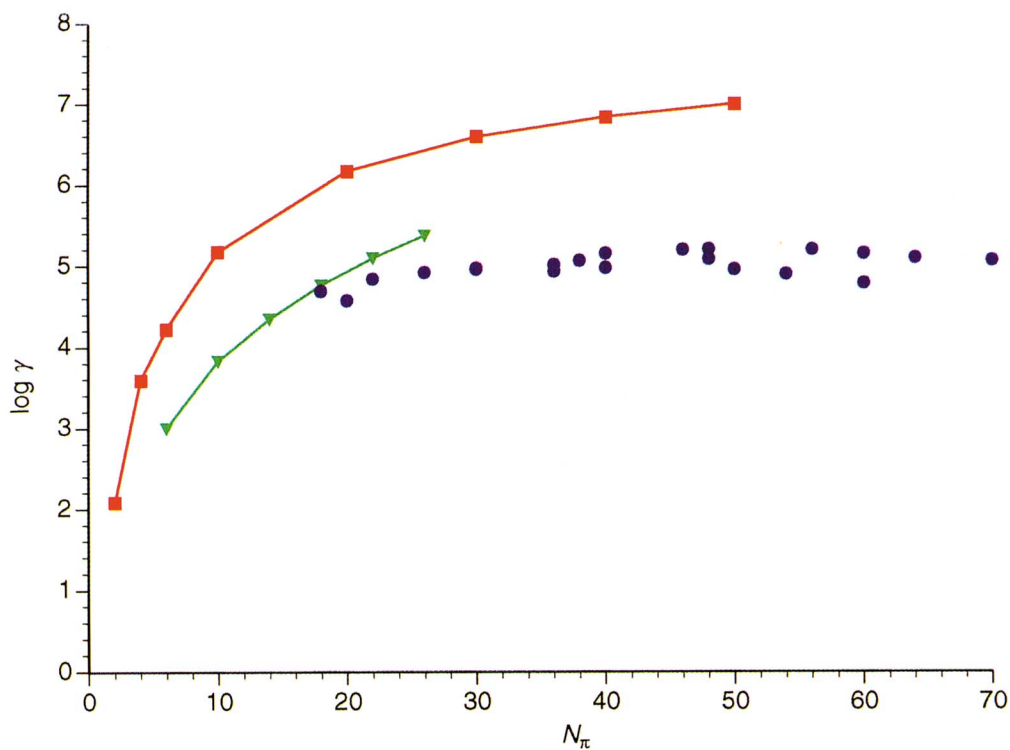


Fig. 3 A graph of  $N_\pi$  against  $\log \gamma$ . The red curve corresponds to the *cis*-polyacetylenes, the green line to the linear acenes, and the scattered blue points the group of curved aromatic molecules depicted in Fig. 1.

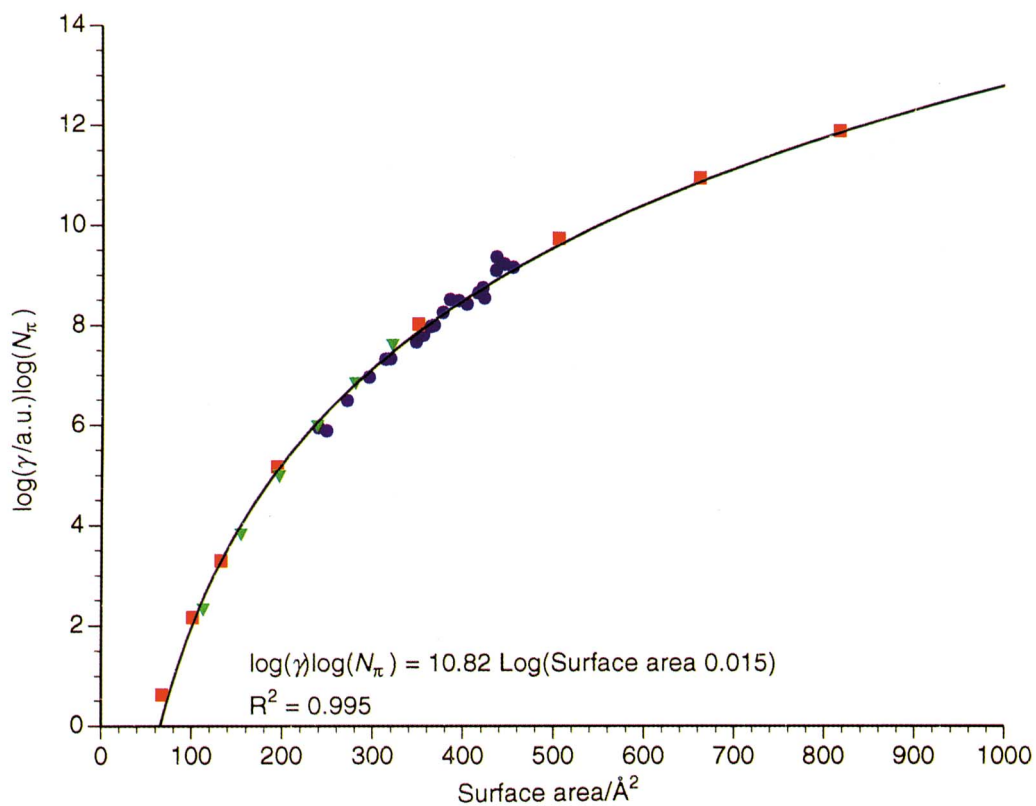
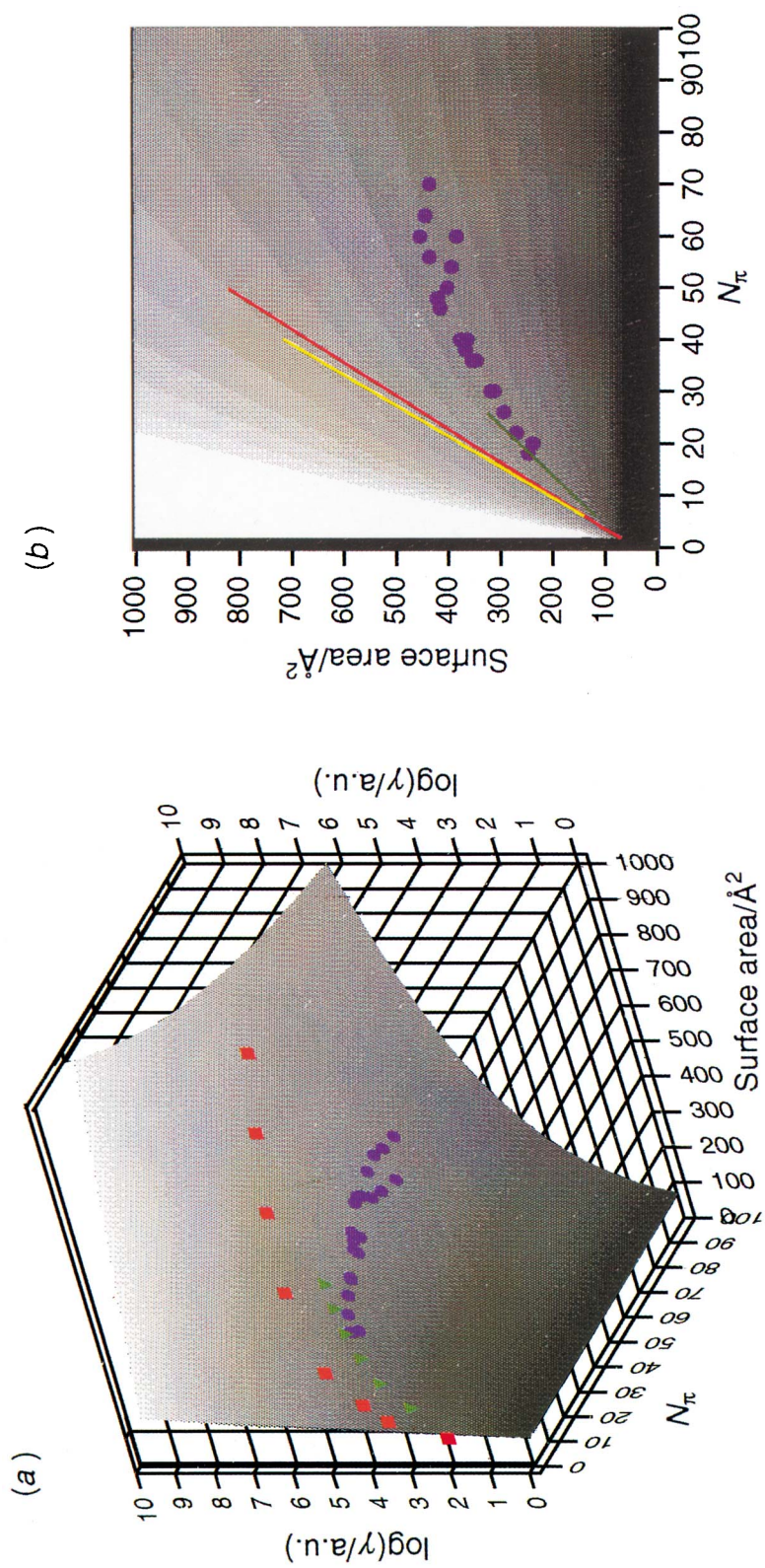


Fig. 4 A graph showing the excellent correlation between surface area and the quantity  $\log \gamma \log N_\pi$ . For colour coding, see the caption for Fig. 3.

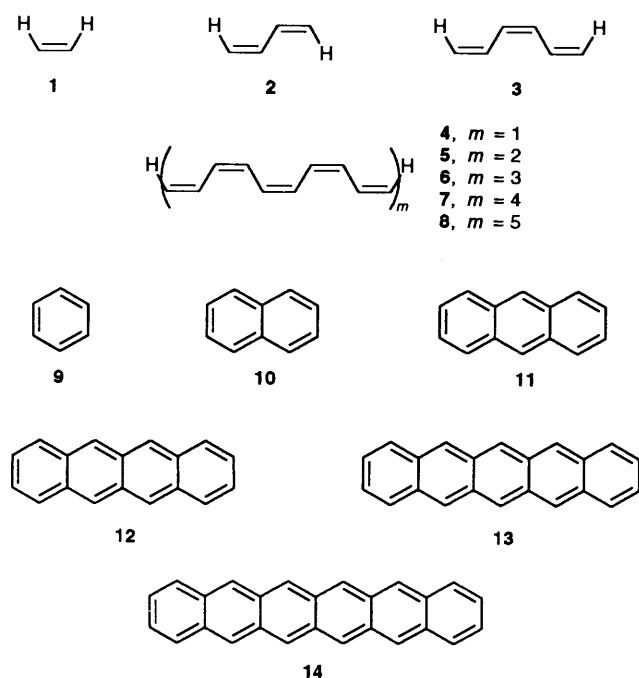


**Fig. 5** Surface plots of surface area vs.  $N_\pi$  vs.  $\log \gamma$ . (a) Shows a side view and (b) shows a top view of the surface. The overlaid yellow line corresponds to the *trans*-polyacetylenes; the rest of the colour coding is described in Fig. 3.

[facing p. 2139]

**Table 1** Calculated values of  $\gamma$  and surface area and the number of  $\pi$  electrons of the hydrocarbons investigated

Entry	$N_\pi$	Surface area/ $\text{\AA}^3$	$\gamma/\text{au}$ (MOPAC)	$\gamma/\text{au}$ (from curve)	Difference in $\gamma$ (%)
1	2	67.2	$1.20 \times 10^2$	$2.41 \times 10^0$	-98
2	4	101.0	$3.88 \times 10^3$	$2.35 \times 10^3$	-39
3	6	132.1	$1.66 \times 10^4$	$1.68 \times 10^4$	1
4	10	194.2	$1.47 \times 10^5$	$1.26 \times 10^5$	-14
5	20	350.2	$1.45 \times 10^6$	$1.12 \times 10^6$	-23
6	30	505.7	$3.87 \times 10^6$	$3.15 \times 10^6$	-19
7	40	661.8	$6.77 \times 10^6$	$6.03 \times 10^6$	-11
8	50	816.7	$9.87 \times 10^6$	$9.45 \times 10^6$	-4
9	6	112.2	$9.90 \times 10^2$	$1.75 \times 10^3$	77
10	10	153.9	$6.73 \times 10^3$	$1.02 \times 10^4$	51
11	14	196.0	$2.22 \times 10^4$	$3.08 \times 10^4$	39
12	18	238.1	$5.78 \times 10^4$	$6.70 \times 10^4$	16
13	22	280.0	$1.25 \times 10^5$	$1.20 \times 10^5$	-4
14	26	321.6	$2.38 \times 10^5$	$1.91 \times 10^5$	-20
15	18	248.6	$4.90 \times 10^4$	$9.73 \times 10^4$	99
16	20	239.4	$3.74 \times 10^4$	$4.75 \times 10^4$	27
17	22	271.0	$6.88 \times 10^4$	$9.24 \times 10^4$	34
18	26	295.6	$8.37 \times 10^4$	$1.00 \times 10^5$	20
19	30	313.7	$9.11 \times 10^4$	$9.51 \times 10^4$	4
20	30	319.6	$9.34 \times 10^4$	$1.09 \times 10^5$	17
21	36	347.7	$8.58 \times 10^4$	$1.09 \times 10^5$	27
22	36	355.7	$1.04 \times 10^5$	$1.27 \times 10^5$	22
23	38	367.8	$1.17 \times 10^5$	$1.34 \times 10^5$	15
24	40	364.0	$9.56 \times 10^4$	$1.06 \times 10^5$	11
25	40	377.3	$1.43 \times 10^5$	$1.35 \times 10^5$	-5
26	46	416.7	$1.59 \times 10^5$	$1.68 \times 10^5$	6
27	48	423.0	$1.22 \times 10^5$	$1.62 \times 10^5$	33
28	48	421.5	$1.60 \times 10^5$	$1.59 \times 10^5$	0
29	50	403.7	$9.15 \times 10^4$	$1.06 \times 10^5$	16
30	54	394.7	$7.98 \times 10^4$	$7.39 \times 10^4$	-7
31	56	436.6	$1.61 \times 10^5$	$1.25 \times 10^5$	-23
32	60	385.1	$6.13 \times 10^4$	$4.76 \times 10^4$	-22
33	60	455.0	$1.43 \times 10^5$	$1.31 \times 10^5$	-8
34	64	446.0	$1.28 \times 10^5$	$9.67 \times 10^4$	-24
35	70	437.0	$1.19 \times 10^5$	$6.75 \times 10^4$	-43



not members of a series of linear oligomers, are completely unaddressed by this type of analysis. For example, the overlaid scatter plot of the curved aromatics in Fig. 3 shows only a narrow range of  $\gamma$  values, almost independent of the number of  $\pi$  electrons,  $N_\pi$ .

**Table 2** Comparison of experimental and calculated values of  $\gamma$  for *trans*-polyacetylenes

Molecular formula	$N_\pi$	VEH/SOS results/au	Experimental results/au	Surface area results/au
$\text{C}_8\text{H}_{10}$	8	$1.22 \times 10^4$	$9.93 \times 10^4$	$4.49 \times 10^4$
$\text{C}_{10}\text{H}_{12}$	10	$4.22 \times 10^4$	$1.97 \times 10^5$	$1.05 \times 10^5$
$\text{C}_{12}\text{H}_{14}$	12	$1.10 \times 10^5$	$3.57 \times 10^5$	$2.07 \times 10^5$
$\text{C}_{14}\text{H}_{16}$	14	$2.39 \times 10^5$	$5.56 \times 10^5$	$3.41 \times 10^5$
$\text{C}_{16}\text{H}_{18}$	16	$4.50 \times 10^5$	$7.94 \times 10^5$	$5.30 \times 10^5$
$\text{C}_{18}\text{H}_{20}$	18	$7.63 \times 10^5$	$1.13 \times 10^6$	$7.65 \times 10^5$
$\text{C}_{20}\text{H}_{22}$	20	$1.19 \times 10^6$	$1.65 \times 10^6$	$1.02 \times 10^6$
$\text{C}_{22}\text{H}_{24}$	22	$1.75 \times 10^6$	$2.18 \times 10^6$	$1.35 \times 10^6$

In a series of linear conjugated oligomers, the number of  $\pi$  electrons is roughly proportional to the length, the surface area and the volume. However, choice of an inappropriate term will lead to a family of curves when different oligomer series are compared, as shown in Fig. 3. In the case of 'higher-dimensional' molecules, the problem becomes even more acute: the concept of length (particularly conjugation length) becomes ill-defined in molecules like buckminsterfullerene,  $\text{C}_{60}$ . Rather than the length, a measurement of higher dimension such as the surface area\* of the molecules may be more appropriate for the dependence. Since  $\gamma$  must also depend on  $N_\pi$  independent of surface area† we seek a relation involving both quantities. The graph in Fig. 4 shows the excellent correlation between the surface area of the molecules, and the quantity  $\log(N_\pi) \log(\gamma)$ . Table 1 shows the values for  $\gamma$  calculated from this correlation. The smallest members of each series of compounds show deviations of up to a factor of two between these and the MOPAC results (for example  $\gamma$  for ethene is twice as large as it should be). In these cases, which have very small values of  $\gamma$ , deviations in the correlation as well as the limit of the numerical accuracy of the MOPAC calculations cause errors on the order of  $\gamma$ , which lead to the discrepancy. In the other cases the values are in good agreement with those calculated by MOPAC.

In order to demonstrate the validity of these data with respect to experimental results, a number of comparisons were made between  $\gamma$  as predicted from surface area measurements and empirical data. Table 2 shows the experimental values of  $\gamma$  for a series of *trans*-polyacetylenes,<sup>13</sup> along with the results of VEH/SOS calculations by Shuai and Brédas,<sup>5a</sup> and values derived from the surface area correlation. As Table 2 shows, these latter results (which were not used in deriving the correlation) are in excellent agreement both qualitatively and quantitatively with the experimental results and show comparable deviations to the values derived from the far more time consuming VEH/SOS calculations. Surprisingly, despite the deviation of the surface area derived values from those of the MOPAC calculation in the smallest molecules, these values are in excellent agreement with experimental data. Table 3 shows experimental<sup>14</sup> and surface area derived data for oligo-*p*-phenylenes. In this case also, agreement between the two sets is very good.

From these comparisons it is clear that the relationship can be used to estimate the second order hyperpolarisabilities of conjugated hydrocarbons to at least the same level of accuracy as semiempirical methods.

In order to visualise the effect of surface area (SA) and  $N_\pi$  on

\* The surface areas were obtained by calculation of the Connolly solvent accessible surface of the MOPAC minimised molecules with a probe radius of 0.1  $\text{\AA}$  using the Insight II software package from Biosym, San Diego.<sup>12</sup>

† Aliphatic molecules have far lower values of  $\gamma$  than their aromatic 'counterparts'.

**Table 3** Comparison of  $\gamma$  for oligo-paraphenylenes derived from experimental results and the surface area correlation

Number of rings	$N_\pi$	Experimental results/au	Surface area results/au
2	12	$5.76 \times 10^4$	$2.94 \times 10^4$
3	18	$1.69 \times 10^5$	$1.24 \times 10^5$
5	30	$4.17 \times 10^5$	$5.69 \times 10^5$

$\gamma$ , surface plots of SA vs.  $N_\pi$  vs.  $\log \gamma$  were generated from the equation fit in Fig. 4. These are shown in Fig. 5. The graphs highlight the advantage of considering both the number of  $\pi$  electrons and the surface area in the design of compounds showing high  $\gamma$ . In contrast to the apparently independent plots shown in Fig. 3, the surface in Fig. 5 allows rationalisation and comparison of the different development in  $\gamma$  of unrelated series of oligomers.

The effect on  $\gamma$  of two particular design scenarios will be examined in detail: the case of a series of linear oligomers, where  $N_\pi \propto SA$ ; and formation of cations (where  $N_\pi$  decreases while SA remains nearly constant).

*Linear Oligomers, where  $N_\pi \propto SA$ .*—In this situation the evolution of  $\gamma$  with increasing  $N_\pi$  can be seen by taking planar slices through the surface in Fig. 5 at  $SA = kN_\pi$  (where  $k$  is a characteristic constant of each oligomer series). The plots of the *cis*-polyacetylenes and acenes in Fig. 3 show the form of these graphs. Examination of Fig. 5(b) shows clearly that in the saturation limit the lines corresponding to these series (as well as that of the *trans*-polyacetylenes) are no longer crossing the gradients of the slope, but rather moving along them. That is, they are circling the 'log  $\gamma$  hill' rather than ascending it. It can be seen that on a surface of this form, all linear polymers will have such a saturation limit, and that the onset will be inversely related to the surface area per  $\pi$  electron ( $SA/N_\pi = k$ ). The experimental observation that the *trans* form of a particular polyacetylene shows higher  $\gamma$  than the *cis* form is accounted for by the differences in surface areas for the two isomers. This is in agreement with Garito's observation<sup>15</sup> that plots of polymer length against  $\gamma$  yield a single curve for *cis* and *trans* polyacetylenes.

*The Formation of Cations.*—The graphs in Fig. 5 show that for a hypothetical molecule of given surface area, increasing the number of  $\pi$  electrons causes a decrease in  $\gamma$ . This is identical to the behaviour of  $\gamma$  in the free-electron model as derived by Ducuing.<sup>16</sup> In that model, the linear polymers are approximated by a one-dimensional box (in which case the change in surface area is proportional to the change in length). For any given box length, increasing the number of electrons causes a decrease in  $\gamma$ .<sup>\*</sup> The graphs in Fig. 5 also agree with the free-electron model

by indicating an increase in  $\gamma$  for fixed  $N_\pi$  and increasing surface area. Analysis of this behaviour from a practical standpoint suggests that delocalised cationic systems (whose surface areas are only changed slightly from those of their neutral parents) will show large third-order NLO responses. A concrete example of such a system is the crystal violet cation which has been shown to possess a surprisingly high  $\gamma$  value.<sup>15</sup>

In summary, the relationship between  $\gamma$  and surface area in conjugated hydrocarbons of widely differing topologies has been identified. This can be viewed as a generalisation of the relationship between  $\gamma$  and length in linear oligomers. Because of its more general nature, it can be used in a predictive manner in the design of new compounds with good NLO responses. We are currently examining the extension of these results to include heteroatoms, as well as investigating their practical application to the design of materials with a high  $\gamma$  value.

### Acknowledgements

The author wishes to thank Professor F. Diederich for generous support and helpful discussions.

### References

- 1 T. H. Maimann, *Nature*, 1960, **187**, 493.
- 2 (a) J. L. Brédas, C. Adant, P. Tackx and A. Persoons, *Chem. Rev.*, 1994, **94**, 243; (b) *Nonlinear Optical Properties of Organic Molecules and Crystals*, ed. D. S. Chemla and J. Zyss, Academic Press, New York, 1987, vols. 1 and 2; (c) P. N. Prasad and D. J. Williams, *Introduction to Nonlinear Optical Effects in Molecules and Polymers*, Wiley, New York, 1991; (d) S. H. Nalwa, *Adv. Mater.*, 1993, **5**, 341.
- 3 K. C. Rustagi and J. Ducuing, *Opt. Commun.*, 1974, **10**, 258.
- 4 D. Beljonne, Z. Shuai and J. L. Brédas, *J. Chem. Phys.*, 1993, **98**, 8819.
- 5 (a) Z. Shuai and J. L. Brédas, *Phys. Rev. B*, 1992, **46**, 4395; (b) Z. Shuai and J. L. Brédas, *Phys. Rev. B*, 1991, **44**, 5962.
- 6 N. Matsuzawa and D. A. Dixon, *J. Phys. Chem.*, 1992, **96**, 6241.
- 7 J. J. P. Stewart, QCPE Program 455, 1983; version 6.00, 1990.
- 8 J. J. P. Stewart, *J. Comput.-Aided Mol. Des.*, 1990, **4**, 1.
- 9 J. J. P. Stewart, *J. Comput. Chem.*, 1989, **10**, 209; 221.
- 10 J. Baker, *J. Comput. Chem.*, 1986, **7**, 385.
- 11 H. A. Kurtz, J. J. P. Stewart and K. M. Dieter, *J. Comput. Chem.*, 1990, **11**, 82.
- 12 (a) M. L. Connolly, *J. Appl. Crystallogr.*, 1983, **16**, 548; (b) M. L. Connolly, *Science*, 1983, **221**, 709.
- 13 G. S. W. Craig, R. E. Cohen, R. R. Schrock, R. J. Silbey, G. Pucetti, I. Ledoux and J. Zyss, *J. Am. Chem. Soc.*, 1993, **115**, 860.
- 14 M. T. Zhao, M. Samoc, B. P. Singh and P. N. Prasad, *J. Phys. Chem.*, 1989, **93**, 7916.
- 15 J. R. Hefflin, K. Y. Wong, O. Zamani-Khamiri and A. F. Garito, *Phys. Rev. B*, 1988, **38**, 1574.
- 16 J. Ducuing, in *Nonlinear Spectroscopy*, ed. N. Bloembergen, North Holland, Amsterdam, 1977, p. 276.
- 17 J. L. Brédas, F. Meyers, in *Organic Materials for Nonlinear Optics III*, ed. G. J. Ashwell and D. Bloor, Royal Society Chemistry, London, 1993, p. 129.

Paper 4/02669A

Received 5th May 1994

Accepted 29th June 1994

\* This behaviour was rationalised in terms of the Band Theory, wherein for a given box length, increasing the number of electrons causes the filling of the Fermi sea and an associated increase in the energy of the first excited state, thus leading to the decrease in  $\gamma$ .<sup>17</sup>